Acetylcholinesterase modulates Presenilin-1 levels and γ-secretase activity

María-Letizia Campanari[1,2], María-Salud García-Ayllón[1,2,3], Olivia Belbin[2,4]; Joan Galcerán[1], Alberto Lleó[2,4], and Javier Sáez-Valero[1,2]

[1]Instituto de Neurociencias de Alicante, Universidad Miguel Hernández-CSIC, Sant Joan d'Alacant, E-03550, Spain; [2]Centro de Investigación Biomédica en Red sobre Enfermedades Neurodegenerativas (CIBERNED), Spain; [3]Unidad de Investigación, Hospital General Universitario de Elche, FISABIO, Elche, Spain; [4]Memory Unit, Neurology Department, Hospital de la Santa Creu i Sant Pau, Barcelona, Spain.

To whom correspondence should be addressed: j.saez@umh.es

Tel.:+34 965919580, Fax:+34 965919561.

Running title: *AChE influences PS1*

Key Words: Alzheimer's disease, γ-secretase, presenilin 1, acetylcholinesterase, inhibitor.

Number of words, Abstract: ~ 210 w **Manuscript:** ~ 4370 w

Number of Figures: 5 Figures + 1 Supplementary Figure

Abstract

The cholinergic enzyme acetylcholinesterase (AChE) and the catalytic component of the γ-secretase complex, presenilin-1 (PS1), are known to interact. In this study, we investigate the consequences of AChE-PS1 interactions, particularly the influence of AChE in PS1 levels and γ-secretase activity. PS1 is able to co-immunoprecipitate all AChE variants (AChE-R and AChE-T) and molecular forms (tetramers and light subunits) present in the human brain. Over-expression of AChE-R or AChE-T, or their respective inactive mutants, all trigger an increase in PS1 protein levels. The AChE specie capable of triggering the biggest increase in PS1 levels is a complex of AChE with the membrane anchoring subunit proline-rich membrane anchor (PRiMA), which restricts the localization of the resulting AChE tetramer to the outer plasma membrane. Incubation of cultured cells with soluble AChE demonstrates that AChE is able to increase PS1 at both the protein and transcript levels. However, the increase of PS1 caused by soluble AChE is accompanied by a decrease in γ-secretase activity as shown by the reduction of the processing of the β-amyloid precursor protein. This inhibitory effect of AChE on γ-secretase activity was also demonstrated by directly assessing accumulation of CTF-APP in cell-free membrane preparations incubated with AChE. Our data suggest that AChE may function as an inhibitor of γ-secretase activity.

Introduction

Acetylcholinesterase (AChE) is a key enzyme in the cholinergic nervous system. Due to its physiological role of hydrolyzing acetylcholine and supporting neurotransmission, this enzyme has been extensively investigated and targeted for pharmacological intervention. In Alzheimer's disease (AD), the loss of forebrain cholinergic neurons is accompanied by a progressive decline in acetylcholine [1,2]. Deficits in cholinergic function most likely contribute to AD symptoms, affecting cognition, behaviour and daily living activities. Although changes in other elements of the cholinergic system [3,4] are also involved in AD, current AD therapy is mostly focused on inhibitors of AChE [5,6]. Thus, randomized clinical trials have demonstrated the efficacy of AChE inhibitors across a wide range of AD severity [7].

Many studies suggest that AChE could have alternative functions unrelated to cholinergic neurotransmission [8-12], or its catalytic activity [13-15]. AChE exists as different variants derived from alternative RNA splicing, generating different polypeptide encoding transcripts with the same catalytic domain but distinct C-terminal peptides, which determine the ability of the molecule to form oligomers [16]. These different transcripts may also influence protein-protein interactions. In the brain, the major T-transcript encodes subunits which produce monomeric (G_1) and tetrameric (G_4, the cholinergic species) AChE forms; while the R-transcript, that is normally present at low levels, encodes monomeric soluble subunits [17]. The particular subcellular distribution of each AChE species allows for its interaction with specific proteins.

Brain accumulation of the β-amyloid peptide (Aβ) is a critical feature of AD pathogenesis. Aβ is the main component of extracellular amyloid plaques and is generated by processing of the larger transmembrane β-amyloid precursor protein (APP) [18,19], by the successive action of two proteolytic enzymes, β-secretase and γ-secretase [20]. We have previously identified presenilin-1 (PS1), the active component

of the γ-secretase complex [21], as an interacting protein of AChE [22]. We have also shown that genetic modulation of AChE expression influences PS1 levels [23].

In this study, we further explore the consequences of AChE-PS1 interactions. We investigate which AChE variant and molecular form influences PS1 levels and if the AChE enzymatic activity is responsible for modulating PS1 expression. Finally we address whether altered levels of PS1, triggered by AChE, induce changes in γ-secretase activity.

Material and methods

Cell Cultures

Chinese Hamster Ovary (CHO) cells were grown in D-MEM+GlutaMAX™-I (Dulbecco's Modified Eagle medium; Gibco®, Life technologies Paisley, UK) supplemented with 10% fetal bovine serum (FBS, Gibco) and 1% penicillin/streptomycin solution (P/S; 100 U/mL) (Gibco). Cells were seeded at a density of 8×10^5 cells on 35 mm tissue culture dishes and were transfected the following day with plasmid cDNA using Lipofectamine™ 2000 (Invitrogen™, Life technologies Paisley, UK) according to the manufacturer's instructions. The plasmids employed encoded either human AChE-T (4µg) or AChE-R (1µg) under the cytomegalovirus (CMV) promoter-enhancer (a generous gift from Dr. H. Soreq, The Institute of Life Sciences, The Hebrew University of Jerusalem, Jerusalem, Israel). The PCI "empty" vector (Promega, Madison, USA) served as negative control. After 48 hours of transfection, cells were washed with phosphate-saline buffer (PBS) and resuspended in 120 µL ice-cold extraction buffer: 50 mM Tris-HCl, pH 7.4 / 150 mM NaCl / 5 mM EDTA / 1% (w/v) Nonidet P-40 / 0.5% (w/v) Triton X-100 supplemented with a cocktail of protease inhibitors. Cell lysates were then sonicated and centrifuged at 70,000×*g* at 4 ºC for 1 hour. The supernatants were collected and frozen at -80ºC until biochemical analysis. Alternatively, AChE-T and AChE-R were over-expressed in SH-SY5Y neuroblastoma cells, grown as described elsewhere [23].

To determine if localization of AChE in the plasma membrane influences PS1 levels, CHO cells were seeded at a density of 6×10^5 cells on 35 mm tissue culture dishes and transfected with 2µg of AChE-T cDNA, with or without 2µg of PRiMA plasmid cDNA using Lipofectamine™ 2000. The cDNA encoding the mouse PRiMA isoform I tagged with an HA epitope (YPYDVPDYA) inserted before the stop codon at the C-terminus [24], was a generous gift from Dr. K.W.K. Tsim (The Hong Kong University

of Science and Technology, Hong Kong, China). The cells were collected for analysis 48 hours after the transfection.

To estimate the AChE activity at the plasma membrane, CHO cells previously transfected with AChE-T cDNA (2µg) with or without 2µg of PRiMA plasmid cDNA, were treated with the AChE inhibitor tacrine, 10µM (Sigma-Aldrich, St. Louis, MO, USA). Forty-eight hours after transfection, cells were washed with PBS and intact cultured cells were measured for AChE activity using a modified microassay version of the colorimetric Ellman's method [25].

CHO cells stably overexpressing wild-type human PS1 and wild-type APP (CHO-PS70, a generous gift from Dr. D. Selkoe, Brigham and Women's Hospital, Boston; see ref. 26), were grown in Opti-MEM® (Gibco) containing 10% FBS, 1% P/S and additionally supplemented with 200 µg/ml G418 and 2.5 µg/ml Puromycin (Sigma-Aldrich). These cells were treated with soluble AChE from *Electrophorus electricus* (*eel*-AChE; Sigma-Aldrich) or vehicle (PBS) for 18 hours, solubilized, and C-terminal fragments of APP (CTF-APP) quantified by Western blot, and PS1 transcript levels by quantitative RT-PCR (*q*RT-PCR).

Generation of inactive catalytic mutants of AChE

Catalytically inactive species of AChE-R and AChE-T were generated by site-directed mutagenesis using the QuickChange^{TM} site directed mutagenesis Kit (Stratagene, La Jolla, CA, USA) according to the manufacturer's protocol. AChE activity was removed in the plasmid cDNA of both active AChE-R and AChE-T by replacing the centre active serine^{200} with valine [27].

Inactive mutants (*im*AChE-T or *im*AChE-R; 3µg of the cDNAs) were overexpressed in CHO cells using the Lipofectamine™ 2000 protocol. Cells were harvested and solubilized after 48 hours. Protein AChE over-expression was assessed

by Western blot, while the inactive character of the mutants was determined by measuring AChE activity levels.

Human brain samples

Samples of adult brain prefrontal cortex from non-demented subjects (three cases, 2 females and 1 male, 58 ±3 years) were obtained from the Banco de Tejidos, Fundación CIEN (Madrid, Spain). Tissues stored at -80°C were thawed gradually at 4°C and small pieces of prefrontal cortex were homogenized (10% w/v) in ice-cold 50 mM Tris-HCl (pH 7.4)-500 mM NaCl-5 mM EDTA-1% (w/v) Nonidet P-40-0.5% (w/v) Triton X-100 supplemented with a cocktail of protease inhibitors. The homogenates were sonicated and centrifuged at 70,000×*g* at 4°C for 1 hour; the supernatant was collected, aliquoted and frozen at -80°C until use. This study was approved by the local ethics committees and carried out in accordance with the Declaration of Helsinki.

AChE enzyme assay and protein determination

A modified microassay version of the colorimetric Ellman's method was used to measure AChE [25]. One mU of AChE activity was defined as the number of nmoles of acetylthiocholine hydrolyzed per minute at 22°C. Total protein concentrations were determined using the BCA Protein Assay Kit (Thermo Scientific, Rockford, IL, USA).

Analysis of AChE molecular forms

Molecular forms of AChE were separated according to their sedimentation coefficients by ultracentrifugation on continuous 5% to 20% (w/v) sucrose gradients containing 0.5% (w/v) Triton X 100, as previously described [25,28]. Enzymes of known sedimentation coefficient, bovine liver catalase (11.4S) and calf intestinal alkaline phosphatase (6.1S) were used in the gradients to identify individual AChE forms (G_4 = tetramers; G_2 =dimers; G_1 =monomers).

Preparation of membrane fractions and γ-secretase activity assay

Alternatively, for analysis of γ-secretase activity cell membrane preparations were used [29]. CHO-PS70 cells were washed in PBS, harvested and homogenized using a mechanical pestle homogenizer in buffer containing 10 mM KCl and 10 mM HEPES, pH 7.0, supplemented with a protease inhibitor cocktail. The cell homogenates were centrifuged at 1,000×*g* for 10 min, and the post-nuclear supernatant was obtained after centrifugation at 100,000×*g* for 1 hour. Membrane fractions were resuspended in buffer containing 20 mM Hepes pH 7.0, 150 mM NaCl, 5 mM EDTA and a protease inhibitor cocktail. Protein concentration was measured by the BCA Protein Assay Kit (Thermo Scientific) and maintained at 3–5 mg/ml. The samples were incubated in the absence or presence of *eel*-AChE (Sigma-Aldrich) or the γ-secretase inhibitor DAPT, N-[N-(3,5-difluorophenacetyl)-l-alanyl]-S-phenylglycine t-butyl ester (Calbiochem), at 37ºC for 16 hours. γ-Secretase activity was assessed by measuring the levels of CTF-APP and the CTF of another γ-secretase substrate, the apolipoprotein E receptor 2 or ApoER2 [30] by Western blotting.

Western blot

Samples from cell lysates or brain extracts (30 to 50 μg of protein, equal amount in each lane) were resolved by electrophoresis on 10% SDS-polyacrylamide slab gels (SDS-PAGE) under fully reducing conditions. Samples were denatured at 50°C for 15 minutes (PS1) or 98°C for 7 minutes (all the other proteins). For blue-native gel electrophoresis, samples were analyzed as previously described [31], and NativeMark™ Unstained Protein Standards (Life Technologies) were used as molecular weight markers. Following electrophoresis, proteins were blotted onto nitrocellulose membranes (Schleider & Schuell Bioscience GmbH, Dassel, Germany), and membranes were blocked with 5% nonfat milk. The membranes were probed with the following primary antibodies: anti-CTF-APP (Sigma-Aldrich), anti-CTF apolipoprotein E receptor 2 (ApoER2; Abcam), anti-N-terminal PS1 (Calbiochem®, Merck KGaA, Darmstadt, Germany), anti- PEN2 (presenilin enhancer 2; from Sigma), anti-AChE antibody N-19 (Santa Cruz Biotech), an anti-AChE antibody raised to the unique C-terminus of human AChE-R (also a generous gift from Dr. H. Soreq), and anti-glyceraldehyde 3-phosphate dehydrogenase (GAPDH) (Abcam, Cambridge, UK). Western blots for different antibodies were performed individually, to avoid re-using blots. The blots were then incubated with the corresponding secondary antibody conjugated to horseradish peroxidase and the signal was detected using SuperSignal West Femto Chemiluminescent Substrate (Thermo Scientific) in a Luminescent Image Analyzer LAS-1000 Plus (Fujifilm, Tokyo, Japan). For semi-quantitative analysis, the intensity of bands was measured by densitometry with the Science Lab Image Gauge v4.0 software provided by Fujifilm. Protein levels were normalized to GAPDH.

PS1 immunoprecipitation

Brain extracts were pre-cleared by incubation with protein A-Sepharose (Sigma-Aldrich) for 2 hours at 4°C. Immunoprecipitations were performed at 4°C by first incubating 800 µg of protein overnight with the N-terminal PS1 antibody 98/1 (a generous gift form J. Culvenor, Department of Pathology, The University of Melbourne, Australia) previously coupled to protein A-Sepharose by dimethyl pimelimidate dihydrochloride (Sigma-Aldrich). Precipitated proteins were washed with PBS and eluted with 0.1M glycine buffer at pH 2.5. After pH neutralization, supernatants were denatured in Laemmli sample buffer at 97ºC for 7 min and subjected to SDS-PAGE/Western blotting. Blots were incubated with the anti-AChE antibodies Ab31276 and anti-AChE-R.

RNA isolation and analysis of transcripts by *q*RT-PCR

Total RNA was isolated from control CHO-PS70 cells or cells treated with *eel*-AChE using TRIzol Reagent in the PureLink™ Micro-to-Midi Total RNA Purification System (Invitrogen) according to the manufacturer's protocol. First-strand cDNAs were obtained by reverse transcription of 1 µg of total RNA using the High Capacity cDNA Reverse Transcription Kit (Applied Biosystems; life technologies Paisley, UK), according to the manufacturer's instructions. Quantitative PCR amplification was performed in a StepOne™ Real-Time PCR System (Applied Biosystems) with TaqMan GenExpression Assays (Hs00997789 for PS1 and Hs03929097 for GAPDH) and TaqMan PCR Master Mix. Transcript levels for PS1 were calculated using the relative standard curve method normalized to GADPH.

Co-localization of AChE and PS1

CHO cells were transiently co-transfected with either 500 ng each of PS1-GFP (kindly provided by Dr. O. Berezovska; Massachusetts General Hospital, MA, USA) and AChE-T plasmids or 300 ng of each of PS1-GFP, AChE-T and PRiMA plasmids. Cells were fixed with 4% paraformaldehyde after 24 hours and immunostained for AChE using anti-AChE followed by an Alexa647-tagged secondary antibody (Molecular Probes, Inc, USA). Confocal images were taken with a SP5 confocal microscope (Leica Microsystems GmbH, Wetzlar, Germany) using a 63× objective (4× zoom). Laser power was kept low to avoid crossover between the two channels and to avoid pixel saturation. Confocal images were taken in multiple z planes (1micron apart). Analysis was performed using ImageJ software (v1.46g) [32]. Briefly, channels were thresholded to create a binary image and Manders' co-efficients [33] were calculated using the JACoP JaCoP ImageJ plugin [34]. The Manders' co-efficient corresponds to the fraction of AChE-positive pixels that are also positive for PS1. Images showing the pixels where the two channels co-localize were generated for the binary thresholded images using the Co-localization highlighter ImageJ plugin.

Statistical analysis

Data are expressed as means ± standard error of the mean (SEM). Data were analyzed using SigmaStat (Version 2.0; SPSS Inc.) by Student's t-test (two tailed) or by one-way analysis of variance (ANOVA), followed by Tukey test for pair-wise comparisons. Statistical significance was designated as $p < 0.05$.

Results

Several AChE variants and isoforms interact with PS1

We first investigated whether PS1 antibodies were able to co-precipitate the R and T variants, and G_4 and G_1 AChE-T species (Fig. 1). Human brain cortex samples were immunoprecipitated using an anti-PS1 antibody, and the bound fraction was analysed by Western blotting using different anti-AChE antibodies raised against different C-terminal peptides of R and T AChE variants. Western blot analysis of the immunoprecipitates demonstrated that both AChE subunits, T and R, are potential PS1-interacting proteins (Fig. 1A). In agreement with our previous study (Silveyra et al., 2008), ultracentrifugation in sucrose density gradients confirmed that both peaks corresponding to the major AChE G_4 (tetramers of T subunits) and to the minor light forms (monomers of T, and potentially of R subunits) were decreased after immunoprecipitation with PS1 antibodies (Fig. 1B).

We next examined whether these AChE species influence PS1 levels (Fig. 2A). Over-expression of AChE-T and AChE-R in CHO cells, as monomeric forms, leads to a statistically significant increase in PS1 levels, compared to untransfected cells (Fig. 2A). The differences between AChE-R (67 ±19%) and AChE-T increase (36 ±5%) on PS1 levels is not statistically significant ($p= 0.18$). Over-expression of AChE-T and AChE-R in the neuroblastoma cell line SH-SY5Y yield similar increases in PS1 levels (Supplementary Fig. 1).

Influence of AChE in PS1 levels is not dependent on its catalytic activity

All the molecular forms and variants of AChE have been demonstrated to be virtually equivalent in their catalytic activity [35,36]. We next examined whether the suppression of AChE catalytic activity affects its ability to modulate PS1 levels. As it has been previously shown that mutation of serine^{200} to valine abolishes detectable AChE activity

269 [27], we over-expressed site-directed mutants at serine^{200} for both AChE-T and AChE-
270 R. Over-expression of the inactive mutants, *im*AChE-T and *im*AChE-R resulted in an
271 increase in AChE protein levels, as assessed by Western blotting, with no substantial
272 increase in specific activity (Fig. 2B). However, both inactive mutants were able to
273 induce an increase in PS1 levels (Fig. 2B), indicating that the modulatory capacity of
274 AChE is exerted by a mechanism independent of its catalytic activity.
275
276 **Influence of AChE in PS1 levels is dependent on its subcellular localization**
277 The proline-rich membrane anchor (PRiMA) subunit is a small transmembrane protein
278 that represents a limiting factor for the restricted localization of AChE into the plasma
279 membrane. It transforms monomeric AChE-T into a tetrameric AChE (G_4)-PRiMA
280 complex which anchors to the outer cell surface [37-39]. We examined if co-expression
281 of the PRiMA subunit with AChE-T further affects PS1 levels. A CHO cell line over-
282 expressing AChE-T was co-transfected with the PRiMA subunit. As expected, cells
283 over-expressing AChE and PRiMA produced significant amounts of G_4 AChE in
284 comparison with those over-expressing AChE only (Fig. 3A). Greater AChE activity
285 was detected on the outer cell surface of intact (non-permeabilized) cultured cells over-
286 expressing AChE and PRiMA compared to cells transfected with AChE in the absence
287 of PRiMA (Fig. 3B). Immunocytochemistry was also used to compare the distribution
288 of PS1 and AChE, expressed as a monomer or as a tetrameric PRiMA-linked AChE.
289 Immunofluorescence labelling of cells confirmed localization of PS1 to both the
290 cytoplasmic region and the periphery (plasma membrane) (Fig. 3C, D), a finding
291 consistent with previous reports by us and others [22, 40-42]. In the absence of PRiMA,
292 AChE co-localized with PS1 mainly within the cytoplasmic region (80 ±7% of AChE
293 pixels were also positive for PS1; Fig. 3C). In contrast, in the presence of PRiMA,
294 AChE was, as expected, targeted to the plasma membrane with staining predominantly

295 localized to the cell periphery, with minor cytoplasmic co-localization with PS1 (only
296 50 ±6% of AChE pixels were also positive for PS1; p= 0.03 versus AChE without
297 PRiMA; Fig. 3D). The levels of PS1 in cells over-expressing AChE with PRiMA is
298 higher than in cells over-expressing intracellular AChE alone, while over-expression of
299 PRiMA alone fails to trigger noticeable change in PS1 levels (Fig. 3E). The PRiMA
300 subunit is an accessory partner for the cellular disposition of AChE [39], at the plasma
301 membrane always in the presence of AChE. In conclusion, the AChE induced increase
302 in the levels of PS1 is further augmented by the presence of PRiMA at the plasma
303 membrane.
304
305 **AChE increases PS1 protein and mRNA levels**
306 Our results indicate that the ability of AChE to induce an increase in PS1 levels is not
307 dependent on its C-terminal (variant), oligomerization status (molecular form) or
308 enzymatic activity. The most significant variable which determines how AChE
309 influences PS1 levels is co-localization outside the plasma membrane. We therefore
310 assessed if soluble AChE (a G_4 species from *Electrophorus electricus*, *eel*-AChE) is
311 able to modulate endogenous PS1 levels in untransfected CHO cells. After an 18 hour
312 treatment with soluble *eel*-AChE, the levels of PS1 were significantly increased from
313 0.5±1 to 34±1 mU/mL (Fig. 4A). We next determined whether AChE influences the
314 *PS1* expression by measuring *PS1* mRNA levels by *q*RT-PCR. Levels of the *PS1*
315 transcripts were significantly increased (44 ±1%, p< 0.001) in *eel*-AChE treated cells
316 compared to vehicle control cells (Fig. 4B).
317
318 **AChE inhibits γ-secretase activity**
319 Up-regulation of protein levels as a reaction to inhibition is a recognized phenomenon
320 documented for several proteins [43,44], including AChE [17, 46,47]. To assess if

AChE-mediated PS1 up-regulation is linked to an inhibitory effect of AChE on γ-secretase activity, we treated with *eel*-AChE CHO-PS70 cells, which stably overexpress wild-type human PS1 and wild-type APP and exhibit elevated γ-secretase activity [26]. The potential inhibitory effect of AChE on γ-secretase activity was monitored by measuring the accumulation of APP-CTF levels. Cells were treated for 18 hours with increasing amounts of *eel*-AChE, and levels of APP-CTF were determined in cellular extracts by Western blotting using an antibody raised against the APP C-terminal. A dose-dependent effect of AChE on γ-secretase activity was observed, with increased amount of APP-CTF in treated cells (Fig. 5A). The inhibitory effect of AChE on γ-secretase activity was then determined in membrane preparations isolated from CHO-PS70 cells obtained as described elsewhere [29]. The presence of the γ-secretase complex in these membrane preparations was first confirmed by blue native-PAGE (Fig. 5B). A predominant PS1 immunoreactive band, with a molecular mass of ~450 kDa (closed arrowhead), was detected together with other high molecular mass bands, corresponding to large γ-secretase complexes [48,49]. These bands were also immunoreactive for the γ-secretase component PEN2 (presenilin enhancer 2) [50]. To determine the effect of inhibition of γ-secretase activity on γ-secretase cleavage of APP, cell membranes were incubated at 37ºC for 16 hours in the absence or presence of N-[N-(3,5-difluorophenacetyl)-l-alanyl]-S-phenylglycine t-butyl ester (DAPT), a well-known γ-secretase inhibitor that targets PS1 [51]. The efficiency of 5 μM DAPT to inhibit γ-secretase activity was monitored by measuring the accumulation of APP-CTF in membrane preparations (Fig. 5C). Accumulation of APP-CTF was also observed in membrane preparations incubated with ~34±1 mU/mL of *eel*-AChE (Fig. 5C). The increased levels in the membrane preparation treated with *eel*-AChE of the CTF of ApoER2, another γ-secretase substrate [30], which was not over-expressed in CHO-

346 PS70 cells, served to confirm the decrease in γ-secretase in presence of AChE (Fig. 5C).

347 These results suggest that AChE may act as an inhibitor of γ-secretase activity.

348

Discussion

The cholinergic system has been shown to modulate APP metabolism [52,53] and AChE inhibitors affect amyloid production [54-56]. In turn, different reports have supported the possibility that Aβ may up-regulate AChE [57-61]. While characterization of the functional cross-talk between AChE/cholinergic neurotransmission and APP processing is of major interest, there is currently no consensus on the mechanisms which regulate these reciprocal interactions. Recent evidence demonstrates that cholinergic AChE can be down-regulated in neuronal cell lines by APP independently of secretase activity [62]. However, other studies have reported modulatory effects of AChE inhibitors on α-secretase [63,64] and β-secretase [65-67]. Our previous studies have also described that AChE inhibitors are able to modulate PS1 levels [23].

We have previously explored some of the potential consequences of the interaction between AChE and PS1, and demonstrated that AChE knockdown with siRNA, as well as AChE inhibition, decreased cellular PS1 levels; whereas AChE over-expression exerted an opposing effect [23]. Our previous data also suggested that AChE does not exert its modulatory action on PS1 via a cholinergic mechanism, as the cholinergic agonist carbachol had no effect on PS1 [23]. Hence, the mechanisms employed by AChE to influence APP processing remained unclear. Our present study addresses how AChE influences PS1 expression by examining changes in PS1, at both protein and transcriptional levels, in several conditions where distinct AChE variant and molecular forms have been modulated. We first confirmed that AChE does not exert its modulatory action on PS1 via a cholinergic mechanism since mutant inactive variants also influence PS1 levels.

Although all the AChE variants (R and T) and molecular forms (monomers and tetramers) tested can influence PS1 levels, the AChE species that triggered the major increase in PS1 levels was the PRiMA-linked AChE form. The PRiMA subunit restricts

localization of cholinergic tetrameric AChE to the outer plasma membrane. PS1 and AChE are located in the same intracellular compartments, including perinuclear compartments, but interestingly PRiMA has been shown to restrict AChE localization to the membrane of synapses [68-70]. Similarly, PS1 is targeted to the cell surface as an active γ-secretase complex [71]. However, the subcellular localization of biologically active γ-secretase is still a matter of controversy. Our studies demonstrate that AChE inhibits APP processing catalyzed by γ-secretase in both cells and membrane preparations. The possibility that AChE inhibits cleavage of APP by γ-secretase has been recently suggested [72]. Therefore, we postulated that, under non-pathological conditions, it is the cholinergic species of AChE which likely interacts with PS1, within the active γ-secretase complex, but by a mechanism independent of its catalytic activity.

The mechanisms employed by AChE to influence APP processing remain unclear. Besides the involvement of the catalytic activity of AChE, a direct effect based on protein-protein interaction also seems plausible. Indeed, AChE is much more than a cholinergic enzyme with distinct biological functions than merely hydrolysis of acetylcholine. In this context, excess of enzymatically inactivated brain AChE by transgenic over-expression have demonstrated different biological functions [13-15]. Native AChE is also present in non-cholinergic tissues and shares high sequence similarity with several neural cell adhesion proteins [73]. The presence of a cholinesterase-like domain in non-catalytic proteins structurally related to AChE may reflect its capacity for protein-protein interactions. This cholinesterase-like domain may have adhesive properties [74]. Therefore, AChE may inhibit APP processing by blocking access of γ-secretases to APP. We have recently demonstrated that γ-secretase is involved in the cleavage of PRiMA [75]. Neuroligin-1, a postsynaptic adhesion molecule whose extracellular domain is homologous to AChE, is also cleaved by γ-secretase [76]. In general, the specific requirements for a γ-secretase substrate are

vague, and do not depend on a specific amino acid sequence or on endocytosis [77]. More than 90 type-I integral membrane proteins are known to be potentially cleaved by γ-secretase [78], but which of those are "common" substrates for γ-secretase in physiological conditions remains unclear. We favor the hypothesis that AChE acts as an inhibitor of γ-secretase activity by interacting with PS1. Nonetheless, we can speculate that some potential substrates of γ-secretase, such as PRiMA from the AChE cholinergic complex, are not "common" substrates and only interact under specific physiological conditions, but which results in low catalytic efficiency. Likewise binding of AChE subunits to PS1 may restrict γ-secretase activity, similar to a negative feedback by end-product inhibition. Further extensive research is needed to determine how AChE blocks or interferes with PS1 and γ-secretase activity and which pool of AChE is involved in the process.

In this study we report that an increase in AChE blocks γ-secretase activity. Up-regulation in reaction to inhibition is a recognized phenomenon documented for several proteins [43,44], including AChE [17,45]. Our data suggest that inhibition of PS1 by AChE may initiate a feedback process that leads to up-regulation of PS1. Regarding the pathological condition, AChE activity (particularly the cholinergic specie) is decreased in the AD brain [28, 79-81], therefore impeding its ability to modulate γ-secretase activity. Interestingly, therapy with inhibitors of AChE demonstrated weak disease-modifying effects in AD-treated patients, including modulation of APP expression and metabolism [63, 82-85]. As previously mentioned, the mechanisms employed by AChE inhibitors to influence APP processing remain unclear but may involve multiple mechanisms that vary according to the type of AChE inhibition. Specifically, how AChE inhibitors trigger a decrease in PS1 levels is unclear. However, it is important to note that the positive modulation of AChE inhibitors on APP failed to have a long-term effect in patients [83]. We propose that a limited response to AChE inhibitors may be

427 associated with AChE up-regulation in reaction to chronic inhibition, a feedback
428 process that leads to accumulation of AChE in parallel with the lack of effect on PS1
429 levels [23]. This phenomenon of AChE up-regulation, as a response to anti-AChE
430 therapy, has been confirmed in patients under AChE inhibitor therapy [46,47,86].
431 Nonetheless, the subcellular localization of this new pool of AChE, and therefore the
432 potential to interact with PS1, merits further investigation.

433 In addition, under non-disease conditions AChE occurs as both active and
434 inactive subunits [87,88], and the existence of inactive AChE has been demonstrated in
435 brain [89]. We have recently shown by Western blotting and immunohistochemistry
436 that a prominent pool of enzymatically inactive AChE protein existed in the AD brain
437 [90]. The physiological significance of non-catalytic AChE in brain and how it is
438 affected during pathology and treatment remain unexplored.

439 In conclusion, our data concur with other reports suggesting the regulation of
440 APP processing by AChE. This modulatory effect may involve cholinergic and non-
441 cholinergic mechanisms, independent of the catalytic activity of AChE. We demonstrate
442 a modulation of PS1 by the AChE species via non-cholinergic mechanisms. We also
443 provide evidence that γ-secretase inhibition could result in PS1 up-regulation which is
444 of particular importance for AD therapy [91-93]. Elucidation of the mechanisms
445 involved in the PS1-AChE interaction and reciprocal regulation are important for the
446 optimization of current therapies based on AChE pharmacological interventions.
447

ACKNOWLEDGMENTS

We thank Dr. H. Soreq (The Institute of Life Sciences, The Hebrew University of Jerusalem, Jerusalem, Israel), Dr. D. Selkoe (Brigham and Women's Hospital, Boston, MA, USA) and Dr. O. Berezovska (Massachusetts General Hospital, MA, USA) for the generous gift of the cDNAs and cells. We also thank Marta Pera for technical assistance. MLC is supported by a Consolider-Predoctoral fellowship from the CSIC, Spain. This work was supported by grants from Fundación CIEN-Reina Sofía, Fondo de Investigaciones Sanitarias (FIS; Grant PS09/00684), ISC-III from Spain to JSV; FIS (PI10/00018) to AL; and FIS (CP11/00067) to MSGA. We also thank the support of CIBERNED, ISC-III to JSV and AL.

Disclosure: None of the authors have any actual or potential financial conflicts or conflict of interest related with this study.

References

1. Davies P, Maloney AJ (1976) Selective loss of central cholinergic neurons in Alzheimer's disease. *Lancet* **2**, 1403.

2. Perry EK, Perry RH, Blessed G, Tomlinson BE (1978) Changes in brain cholinesterases in senile dementia of Alzheimer type.Neuropathol Appl Neurobiol **4**, 273-277.

3. Kása P, Rakonczay Z, Gulya K (1997) The cholinergic system in Alzheimer's disease. *Prog Neurobiol* **52**, 511-535.

4. Schliebs R, Arendt T (2011) The cholinergic system in aging and neuronal degeneration. *Behav Brain Res* **221**, 555-563.

5. Giacobini E (2003) Cholinergic function and Alzheimer's disease. *Int J Geriatr Psychiatry* **18**, S1-5.

6. Lleó A, Greenberg SM, Growdon JH (2006) Current pharmacotherapy for Alzheimer's disease. *Annu Rev Med* **57**, 513-533.

7. Di Santo SG, Prinelli F, Adorni F, Caltagirone C, Musicco M (2013) A meta-analysis of the efficacy of donepezil, rivastigmine, galantamine, and memantine in relation to severity of Alzheimer's disease. *J Alzheimers Dis* **35**, 349-361.

8. Massoulié J, Sussman J, Bon S, Silman I (1993) Structure and functions of acetylcholinesterase and butyrylcholinesterase. *Prog Brain Res* **98**, 139-146.

9. Layer PG (1995) Nonclassical roles of cholinesterases in the embryonic brain and possible links to Alzheimer disease. *Alzheimer Dis Assoc Disord* **9**, 29-36.

10. Small DH, Michaelson S, Sberna G (1996) Non-classical actions of cholinesterases: role in cellular differentiation, tumorigenesis and Alzheimer's disease. *Neurochem* **28**, 453-483.

11. Soreq H, Seidman S (2001) Acetylcholinesterase-new roles for an old actor. *Nat Rev Neurosci* **2**, 294-302.

12. Silman I, Sussman JL (2005) Acetylcholinesterase: 'classical' and 'non-classical' functions and pharmacology. *Curr Opin Pharmacol* **5**, 293-302.

13. Sternfeld M, Ming G, Song H, Sela K, Timberg R, Poo M, Soreq H (1998) Acetylcholinesterase enhances neurite growth and synapse development through alternative contributions of its hydrolytic capacity, core protein, and variable C termini. *J Neurosci* **18**, 1240-1249.

14. Dori A, Cohen J, Silverman WF, Pollack Y, Soreq H (2005) Functional manipulations of acetylcholinesterase splice variants highlight alternative splicing contributions to murine neocortical development. *Cereb Cortex* **15**, 419-430.

15. Grisaru D, Pick M, Perry C, Sklan EH, Almog R, Goldberg I, Naparstek E, Lessing JB, Soreq H, Deutsch V (2006) Hydrolytic and non enzymatic functions of acetylcholinesterase comodulate hemopoietic stress responses. *J Immunol* **176**, 27-35.

16. Massoulié J (2002) The origin of the molecular diversity and functional anchoring of cholinesterases. *Neurosignals* **11**, 130-143.

17. Kaufer D, Friedman A, Seidman S, Soreq H (1998) Acute stress facilitates long-lasting changes in cholinergic gene expression. *Nature* **393**, 373-377.

18. Masters CL, Simms G, Weinman NA, Multhaup G, McDonald BL, Beyreuther K (1985) Amyloid plaque core protein in Alzheimer's disease and Down syndrome. *Proc Natl Acad Sci USA* **82**, 4245-4249.

19. Kang J, Lemaire HG, Unterbeck A, Salbaum JM, Masters CL, Grzeschik KH, Multhaup G, Beyreuther K, Müller-Hill B (1987) The precursor of Alzheimer's disease amyloid A4 protein resembles a cell-surface receptor. *Nature* **325**, 733-736.

20. Thinakaran G, Koo EH (2008) Amyloid precursor protein trafficking, processing, and function. *J Biol Chem* **283**, 29615-29619.

514 21. De Strooper B, Iwatsubo T, Wolfe MS (2012) Presenilins and γ-secretase: structure,
515 function, and role in Alzheimer Disease. *Cold Spring Harb Perspect Med* **2**,
516 a006304.
517 22. Silveyra MX, Evin G, Montenegro MF, Vidal CJ, Martínez S, Culvenor JG, Sáez-
518 Valero J (2008) Presenilin 1 interacts with acetylcholinesterase and alters its
519 enzymatic activity and glycosylation. *Mol Cell Biol* **28**, 2908-2919.
520 23. Silveyra MX, García-Ayllón MS, Serra-Basante C, Mazzoni V, García-Gutierrez
521 MS, Manzanares J, Culvenor JG, Sáez-Valero J (2012) Changes in
522 acetylcholinesterase expression are associated with altered presenilin-1 levels.
523 *Neurobiol Aging* **33**, 627.e27-37.
524 24. Chen VP, Choi RC, Chan WK, Leung KW, Guo AJ, Chan GK, Luk WK, Tsim KW
525 (2011) The Assembly of Proline-rich Membrane Anchor (PRiMA)-linked
526 Acetylcholinesterase Enzyme. Glycosylation is required for enzymatic activity but
527 not for oligomerization. *J Biol Chem* **286**, 32948–32961.
528 25. Sáez-Valero J, Tornel PL, Muñoz-Delgado E, Vidal CJ (1993) Amphiphilic and
529 hydrophilic forms of acetyl- and butyrylcholinesterase in human brain. *J Neurosci*
530 *Res* **35**, 678–689.
531 26. Xia W, Zhang J, Kholodenko D, Citron M, Podlisny MB, Teplow DB, Haass C,
532 Seubert P, Koo EH, Selkoe DJ (1997) Enhanced production and oligomerization
533 of the 42-residue amyloid beta-protein by Chinese hamster ovary cells stably
534 expressing mutant presenilins. *J Biol Chem* **272**, 7977-7982.
535 27. Gibney G, Camp S, Dionne M, MacPhee-Quigley K, Taylor P (1990) Mutagenesis
536 of essential functional residues in acetylcholinesterase. *Proc Natl Acad Sci USA*
537 **87**, 7546-7550.
538 28. Sáez-Valero J, Sberna G, McLean CA, Small DH (1999) Molecular isoform
539 distribution and glycosylation of acetylcholinesterase are altered in brain and

cerebrospinal fluid of patients with Alzheimer's disease. *J Neurochem* **72**, 1600-1608.

29. Frånberg J, Karlström H, Winblad B, Tjernberg LO, Frykman S (2010) γ-Secretase dependent production of intracellular domains is reduced in adult compared to embryonic rat brain membranes. *PLoS One* **5**, e9772.

30. Balmaceda V, Cuchillo-Ibáñez I, Pujadas L, García-Ayllón MS, Saura CA, Nimpf J, Soriano E, Sáez-Valero J (2013) ApoER2 processing by presenilin-1 modulates reelin expression. *FASEB J* In press;doi: 10.1096/fj.13-239350.

31. Schägger H, Von Jagow G (1991) Blue native electrophoresis for isolation of membrane protein complexes in enzymatically active form. *Anal Biochem* **199**, 223–231.

32. Schneider CA, Rasband WS, Eliceiri KW (2012) NIH Image to ImageJ: 25 years of image analysis. *Nat Methods* **9**, 671-675.

33. Manders EMM, Verbeek FJ, Aten JA (1993) Measurement of co-localization of objects in dual-colour confocal images. *J Microsc* **169**, 375-382.

34. Bolte S, Cordelieres FP (2006) A guided tour into subcellular colocalization analysis in light microscopy. *J Microsc* **224**, 213-232.

35. Vigny M, Bon S, Massoulié J, Leterrier F (1978) Active-site catalytic efficiency of acetylcholinesterase molecular forms in Electrophorus, torpedo, rat and chicken. *Eur J Biochem* **85**, 317-323.

36. Soreq H, Gnatt A, Loewenstein Y, Neville LF (1992) Excavations into the active-site gorge of cholinesterases. *Trends Biochem Sci* **17**, 353-358.

37. Perrier AL, Massoulié J, Krejci E (2002) PRiMA: the membrane anchor of acetylcholinesterase in the brain. *Neuron* **33**, 275-285.

564 38. Perrier NA, Khérif S, Perrier AL, Dumas S, Mallet J, Massoulié J (2003) Expression
565 of PRiMA in the mouse brain: membrane anchoring and accumulation of 'tailed'
566 acetylcholinesterase. *Eur J Neurosci* **18**, 1837-1847.
567 39. Dobbertin A, Hrabovska A, Dembele K, Camp S, Taylor P, Krejci E, Bernard V
568 (2009) Targeting of acetylcholinesterase in neurons in vivo: a dual processing
569 function for the proline-rich membrane anchor subunit and the attachment domain
570 on the catalytic subunit. *J Neurosci* **29**, 4519-4530.
571 40. Kovacs DM, Fausett HJ, Page KJ, Kim TW, Moir RD, Merriam DE, Hollister RD,
572 Hallmark OG, Mancini R, Felsenstein KM, Hyman BT, Tanzi RE, Wasco W
573 (1996) Alzheimer-associated presenilins 1 and 2: neuronal expression in brain and
574 localization to intracellular membranes in mammalian cells. *Nat Med* **2**, 224-229.
575 41. Huynh DP, Vinters HV, Ho DH, Ho VV, Pulst SM (1997) Neuronal expression and
576 intracellular localization of presenilins in normal and Alzheimer disease brains. *J*
577 *Neuropathol Exp Neurol* 56, 1009-1017.
578 42. Herl L, Lleo A, Thomas AV, Nyborg AC, Jansen K, Golde TE, Hyman BT,
579 Berezovska O (2006) Detection of presenilin-1 homodimer formation in intact
580 cells using fluorescent lifetime imaging microscopy. *Biochem Biophys Res*
581 *Commun* **340**, 668-674.
582 43. Xu L, Kappler CS, Mani SK, Shepherd NR, Renaud L, Snider P, Conway SJ,
583 Menick DR (2009) Chronic administration of KB-R7943 induces up-regulation of
584 cardiac NCX1. *J Biol Chem* **284**, 27265-27272.
585 44. Serfőző Z, Lontay B, Kukor Z, Erdődi F (2012) Chronic inhibition of nitric oxide
586 synthase activity by N(G)-nitro-L-arginine induces nitric oxide synthase
587 expression in the developing rat cerebellum. *Neurochem Int* **60**, 605-615.

588 45. Chiappa S, Padilla S, Koenigsberger C, Moser V, Brimijoin S (1995) Slow
589 accumulation of acetylcholinesterase in rat brain during enzyme inhibition by
590 repeated dosing with chlorpyrifos. *Biochem Pharmacol* **49**, 955-963.
591 46. Darreh-Shori T, Almkvist O, Guan ZZ, Garlind A, Strandberg B, Svensson AL,
592 Soreq H, Hellström-Lindahl E, Nordberg A (2002) Sustained cholinesterase
593 inhibition in AD patients receiving rivastigmine for 12 months. *Neurology* **59**,
594 563-572.
595 47. García-Ayllón MS, Silveyra MX, Andreasen N, Brimijoin S, Blennow K, Sáez-
596 Valero J (2007) Cerebrospinal fluid acetylcholinesterase changes after treatment
597 with donepezil in patients with Alzheimer's disease. *J Neurochem* **101**, 1701-
598 1711.
599 48. Edbauer D, Winkler E, Haass C, Steiner H (2002) Presenilin and nicastrin regulate
600 each other and determine amyloid beta-peptide production via complex formation.
601 *Proc Natl Acad Sci USA* **99**, 8666-8671.
602 49. Kimberly WT, LaVoie MJ, Ostaszewski BL, Ye W, Wolfe MS, Selkoe DJ (2003)
603 Gamma-secretase is a membrane protein complex comprised of presenilin,
604 nicastrin, Aph-1, and Pen-2. *Proc Natl Acad Sci USA* **100**, 6382-6387.
605 50. Kaether C, Haass C, Steiner H (2006) Assembly, trafficking and function of
606 gamma-secretase. *Neurodegener Dis* **3**, 275-283.
607 51. Morohashi Y, Kan T, Tominari Y, Fuwa H, Okamura Y, Watanabe N, Sato C,
608 Natsugari H, Fukuyama T, Iwatsubo T, Tomita T (2006) C-terminal fragment of
609 presenilin is the molecular target of a dipeptidic gamma-secretase-specific
610 inhibitor DAPT (N-[N-(3,5-difluorophenacetyl)-L-alanyl]-S-phenylglycine t-butyl
611 ester). *J Biol Chem* **281**, 14670-14676.

612 52. Nitsch RM, Slack BE, Wurtman RJ, Growdon JH (1992) Release of Alzheimer
613 amyloid precursor derivatives stimulated by activation of muscarinic
614 acetylcholine receptors. *Science* **258**, 304-307.
615 53. Rossner S, Ueberham U, Schliebs R, Pérez-Polo JR, Bigl V (1998) The regulation
616 of amyloid precursor protein metabolism by cholinergic mechanisms and
617 neurotrophin receptor signaling. *Prog Neurobiol* **56**, 541-569.
618 54. Mori F, Lai CC, Fusi F,Giacobini E (1995) Cholinesterase inhibitors increase
619 secretion of APPs in rat brain cortex. *Neuroreport* **6**, 633-636.
620 55. Lahiri DK, Farlow MR, Nurnberger JI Jr, Greig NH (1997) Effects of cholinesterase
621 inhibitors on the secretion of beta-amyloid precursor protein in cell cultures. *Ann*
622 *N Y Acad Sci* **826**, 416-421.
623 56. Zimmermann M, Gardoni F, Marcello E, Colciaghi F, Borroni B, Padovani A,
624 Cattabeni F, Di Luca M (2004) Acetylcholinesterase inhibitors increase ADAM10
625 activity by promoting its trafficking in neuroblastoma cell lines. *J Neurochem* **90**,
626 1489-1499.
627 57. Sberna G, Sáez-Valero J, Beyreuther K, Masters CL, Small DH (1997) The amyloid
628 beta-protein of Alzheimer's disease increases acetylcholinesterase expression by
629 increasing intracellular calcium in embryonal carcinoma P19 cells. *J Neurochem*
630 **69**, 1177-1184.
631 58. Sberna G, Sáez-Valero J, Li QX, Czech C, Beyreuther K, Masters CL, McLean CA,
632 Small DH (1998) Acetylcholinesterase is increased in the brains of transgenic
633 mice expressing the C-terminal fragment (CT100) of the beta-amyloid protein
634 precursor of Alzheimer's disease. *J Neurochem* **71**, 723-731.
635 59. Hu W, Gray NW, Brimijoin S (2003) Amyloid-beta increases acetylcholinesterase
636 expression in neuroblastoma cells by reducing enzyme degradation. *J Neurochem*
637 **86**, 470-478.

638 60. Melo JB, Agostinho P, Oliveira CR (2003) Involvement of oxidative stress in the
639 enhancement of acetylcholinesterase activity induced by amyloid beta-peptide.
640 *Neurosci Res* **45**, 117-127.
641 61. Li G, Klein J, Zimmermann M (2013) Pathophysiological amyloid concentrations
642 induce sustained upregulation of readthroughacetylcholinesterase mediating anti-
643 apoptotic effects. *Neuroscience* **240**, 349-360.
644 62. Hicks DA, Makova NZ, Gough M, Parkin ET, Nalivaeva NN, Turner AJ (2013) The
645 amyloid precursor protein represses expression of acetylcholinesterase in neuronal
646 cell lines. *J Biol Chem* **288**, 26039-26051.
647 63. Zimmermann M, Borroni B, Cattabeni F, Padovani A, Di Luca M (2005)
648 Cholinesterase inhibitors influence APP metabolism in Alzheimer disease
649 patients. *Neurobiol Dis* **19**, 237-242.
650 64. Peng Y, Jiang L, Lee DY, Schachter SC, Ma Z, Lemere CA (2006) Effects of
651 huperzine A on amyloid precursor protein processing and beta-amyloid generation
652 in human embryonic kidney 293 APP Swedish mutant cells. *J Neurosci Res* **84**,
653 903-911.
654 65. Lahiri DK, Chen D, Maloney B, Holloway HW, Yu QS, Utsuki T, Giordano T,
655 Sambamurti K, Greig NH (2007) The experimental Alzheimer's disease drug
656 posiphen [(+)-phenserine] lowers amyloid-beta peptide levels in cell culture and
657 mice. J. Pharmacol. *Exp Ther* **320**, 386-396.
658 66. Fu H, Li W, Luo J, Lee NT, Li M, Tsim KW, Pang Y, Youdim MB, Han Y (2008)
659 Promising anti-Alzheimer's dimer bis(7)-tacrine reduces beta-amyloid generation
660 by directly inhibiting BACE-1 activity. *Biochem Biophys Res Commun* **366**, 631-
661 636.

662 67. Li Q, Wu D, Zhang L, Zhang Y (2010) Effects of galantamine on β-amyloid release
663 and beta-site cleaving enzyme 1 expression in differentiated human
664 neuroblastoma SH-SY5Y cells. *Exp Gerontol* **45**, 842-847.
665 68. Xie HQ, Liang D, Leung KW, Chen VP, Zhu KY, Chan WK, Choi RC, Massoulié J,
666 Tsim KW (2010a) Targeting acetylcholinesterase to membrane rafts: a function
667 mediated by the proline-rich membrane anchor (PRiMA) in neurons. *J Biol Chem*
668 **285**, 11537-11546.
669 69. Xie HQ, Leung KW, Chen VP, Chan GK, Xu SL, Guo AJ, Zhu KY, Zheng KY, Bi
670 CW, Zhan JY, Chan WK, Choi RC, Tsim KW (2010b) PRiMA directs a restricted
671 localization of tetrameric AChE at synapses. *Chem Biol Interact* **187**, 78-83.
672 70. Henderson Z, Matto N, John D, Nalivaeva NN, Turner AJ (2010) Co-localization of
673 PRiMA with acetylcholinesterase in cholinergic neurons of rat brain: an
674 immunocytochemical study. *Brain Res* **1344**, 34-42.
675 71. Kaether C, Lammich S, Edbauer D, Ertl M, Rietdorf J, Capell A, Steiner H, Haass C
676 (2002) Presenilin-1 affects trafficking and processing of beta APP and is targeted
677 in a complex with nicastrin to the plasma membrane. *J Cell Biol* **158**, 551-561.
678 72. Niu X, Zhang X, Xie J, Zhang X (2012) Acetylcholinesterase blocks cleavage of
679 APP by γ-secretase in 293 cells and mouse brain. *Mol Neurodegener* **7**, S11.
680 73. Krejci E, Duval N, Chatonnet A, Vincens P, Massoulié J (1991) Cholinesterase-like
681 domains in enzymes and structural proteins: functional and evolutionary
682 relationships and identification of a catalytically essential aspartic acid. *Proc Natl*
683 *Acad Sci USA* **88**, 6647-6651.
684 74. Darboux I, Barthalay Y, Piovant M, Hipeau-Jacquotte R (1996) The structure-
685 function relationships in Drosophila neurotactin show that cholinesterasic
686 domains may have adhesive properties. *EMBO J* **15**, 4835-4843.

687 75. García-Ayllón MS, Campanari ML, Montenegro MF, Cuchillo-Ibáñez I, Belbín O,
688 Lleó A, Saura CA, Tsim KM, Vidal CJ and Sáez-Valero J (2014) Presenilin-1
689 influences processing of the acetylcholinesterase membrane-binding tail PRiMA.
690 *Neurobiol Aging* in press. doi: 10.1016/j.neurobiolaging.2014.01.147.
691 76. Suzuki K, Hayashi Y, Nakahara S, Kumazaki H, Prox J, Horiuchi K, Zeng M,
692 Tanimura S, Nishiyama Y, Osawa S, Sehara-Fujisawa A, Saftig P, Yokoshima S,
693 Fukuyama T, Matsuki N, Koyama R, Tomita T, Iwatsubo T (2012) Activity-
694 dependent proteolytic cleavage of neuroligin-1. *Neuron* **76**, 410-422.
695 77. Struhl G, Adachi A (2000) Requirements for presenilin-dependent cleavage of notch
696 and other transmembrane proteins. *Mol Cell* **6**, 625-636.
697 78. Lleó A, Saura CA (2011) γ-secretase substrates and their implications for drug
698 development in Alzheimer's disease. *Curr Top Med Chem* **11**, 1513-1527.
699 79. Atack JR, Perry EK, Bonham JR, Perry RH, Tomlinson BE, Blessed G, Fairbairn A
700 (1983) Molecular forms of acetylcholinesterase in senile dementia of Alzheimer
701 type: selective loss of the intermediate (10S) form. *Neurosci Lett* **40**, 199-204.
702 80. Fishman EB, Siek GC, MacCallum RD, Bird ED, Volicer L, Marquis JK (1986)
703 Distribution of the molecular forms of acetylcholinesterase in human brain,
704 alterations in dementia of the Alzheimer type. *Ann Neurol* **19**, 246-252.
705 81. Schegg KM, Harrington LS, Neilsen S, Zweig RM, Peacock JH (1992) Soluble and
706 membrane-bound forms of brain acetylcholinesterase in Alzheimer's disease.
707 *Neurobiol Aging* **13**, 697-704.
708 82. Clarke NA, Soininen H, Gustafson L, Minthon L, Alhainen K, Francis PT (2001)
709 Tacrine may alter APP-like protein levels in the lumbar CSF of Alzheimer
710 patients. *Int J Geriatr Psychiatry* **16**, 1104-1106.
711 83. Borroni B, Colciaghi F, Pastorino L, Pettenati C, Cottini E, Rozzini L, Monastero R,
712 Lenzi GL, Cattabeni F, Di Luca M, Padovani A (2001) Amyloid precursor protein

713 in platelets of patients with Alzheimer disease: effect of acetylcholinesterase
714 inhibitor treatment. *Arch Neurol* **58**, 442-446.
715 83. Basun H, Nilsberth C, Eckman C, Lannfelt L, Younkin S (2002) Plasma levels of
716 Abeta42 and Abeta40 in Alzheimer patients during treatment with the
717 acetylcholinesterase inhibitor tacrine. *Dement Geriatr Cogn Disord* **14**, 156-160.
718 84. Pakaski M, Kasa P (2003) Role of acetylcholinesterase inhibitors in the metabolism
719 of amyloid precursor protein. *Curr Drug Targets CNS Neurol Disord* **2**, 163-171.
720 85. Sobow T, KloszewskaI (2005) Short-term treatment with rivastigmine and plasma
721 levels of Abeta peptides in Alzheimer's disease. *Folia Neuropathol* **43**, 340-344.
722 86. Darreh-Shori T, Hellström-Lindahl E, Flores-Flores C, Guan ZZ, Soreq H,
723 Nordberg A (2004) Long-lasting acetylcholinesterase splice variations in
724 anticholinesterase-treated Alzheimer's disease patients. *J Neurochem* **88**, 1102-
725 1113.
726 87. Stieger S, Brodbeck U, Witzemann V (1987) Inactive monomeric
727 acetylcholinesterase in the low-salt-soluble extract of the electric organ from
728 Torpedo marmorata. *J Neurochem* **49**, 460-467.
729 88. Rotundo RL (1988) Biogenesis of acetylcholinesterase molecular forms in
730 muscle.Evidence for a rapidly turning over, catalytically inactive precursor pool.*J*
731 *Biol Chem* **263**, 19398-19406.
732 89. Chatel JM, Grassi J, Frobert Y, Massoulié J, Vallette FM (1993) Existence of an
733 inactive pool of acetylcholinesterase in chicken brain. *Proc Natl Acad Sci USA* **90**,
734 2476-2480.
735 90. Campanari ML, García-Ayllón MS, Blazquez-Llorca L, Luk WK, Tsim K, Sáez-
736 Valero J (2013) Acetylcholinesterase Protein Level Is Preserved in the
737 Alzheimer's Brain. *J Mol Neurosci* In press;doi: 10.1007/s12031-013-0183-5.

738 91. Wolfe MS (2012) γ-Secretase as a target for Alzheimer's disease. *Adv Pharmacol*
739 **64**, 127-153.
740 92. Wagner SL, Tanzi RE, Mobley WC, Galasko D (2012) Potential use of γ-secretase
741 modulators in the treatment of Alzheimer disease *Arch Neurol* **69**, 1255-1258.
742 93. Gandy S, DeKosky ST (2013) Toward the treatment and prevention of Alzheimer's
743 disease: rational strategies and recent progress. *Annu Rev Med* **64**, 367-383.
744

745 **Figure**

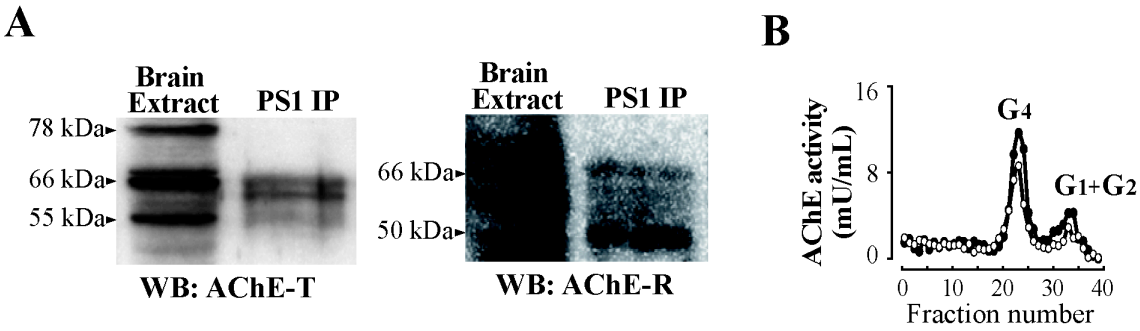

746

747

748 ***Figure 1.*** **PS1 interacts with AChE-T and AChE-R variants**. (**A**) Co-precipitation of
749 PS1 and AChE. Human brain extracts (frontal cortex from three non-demented subjects,
750 mean age 58 ±3 years; one example is shown) were immunoprecipitated with anti-PS1
751 antibody 98/1. PS1-immunoprecipitated proteins (PS1 IP) were immunoblotted with the
752 indicated anti-AChE antibody specific for particular AChE variants (T and R). Extracts
753 incubated with protein A-Sepharose, without antibody, were analyzed in parallel as
754 negative controls (not shown). (**B**) The non-immunoprecipitated fraction was analyzed
755 for molecular forms of AChE by sucrose gradient ultracentrifugation. Approximately 40
756 fractions were collected from the bottom of each tube and assayed for AChE activity.
757 Representative profiles of AChE molecular forms (tetramers: G_4; and light dimers and
758 monomers: G_1+G_2) prior (●) and after (○) immunoprecipitation are shown. Experiments
759 were performed in triplicate.

760

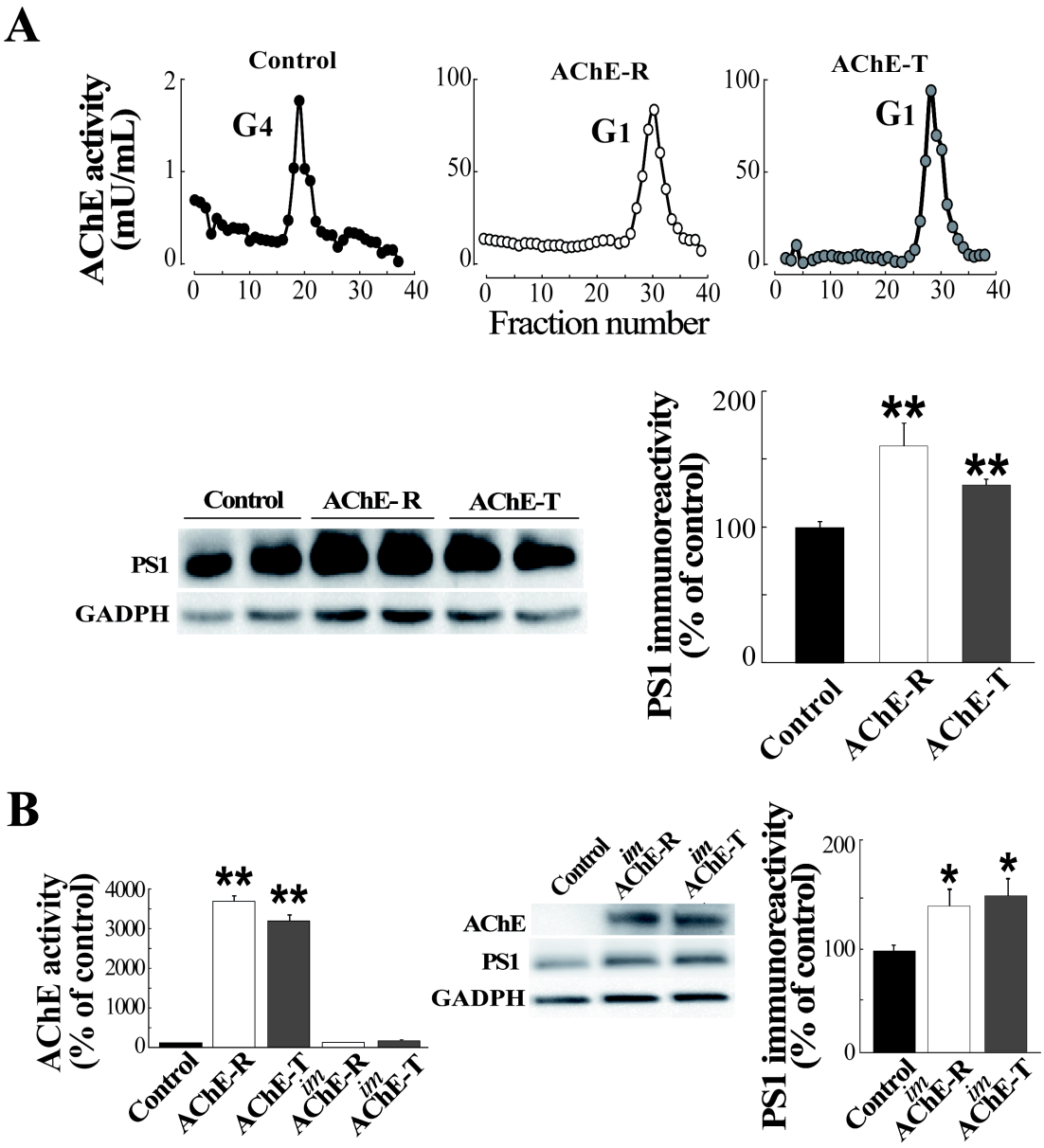

761

762

763 ***Figure 2.*** **PS1 levels are regulated by AChE independent of its enzymatic activity.**

764 (**A**) Representative molecular profiles of AChE and immunodetection of PS1-NTF in

765 CHO cells stably transfected with constructs carrying either the AChE-R or AChE-T

766 cDNA. CHO cells stably transfected with a PCI vector served fas controls (Control).

767 The results were confirmed in three independent experiments. The densitometric

768 quantification of PS1-NTF immunoreactivity is represented. Protein levels were

769 normalized to glyceraldehyde 3-phosphate deydrogenase (GADPH). (**B**) PS1

770 immunodetection and densitometric quantification in cells transfected with the inactive

771 form of AChE-R (*im*AChE-R) and AChE-T (*im*AChE-T). Immunoblots with the anti-
772 AChE antibody N19 antibody confirmed the expression of equal amounts of *im*AChE-R
773 and *im*AChE-T in transfected cells. Columns represent mean ± SEM from three
774 different experiments (n= 12 for each condition). Representative immunoblots are
775 shown. $^{**}p < 0.01$ and $^{*}p < 0.05$, significant difference from the control group.
776

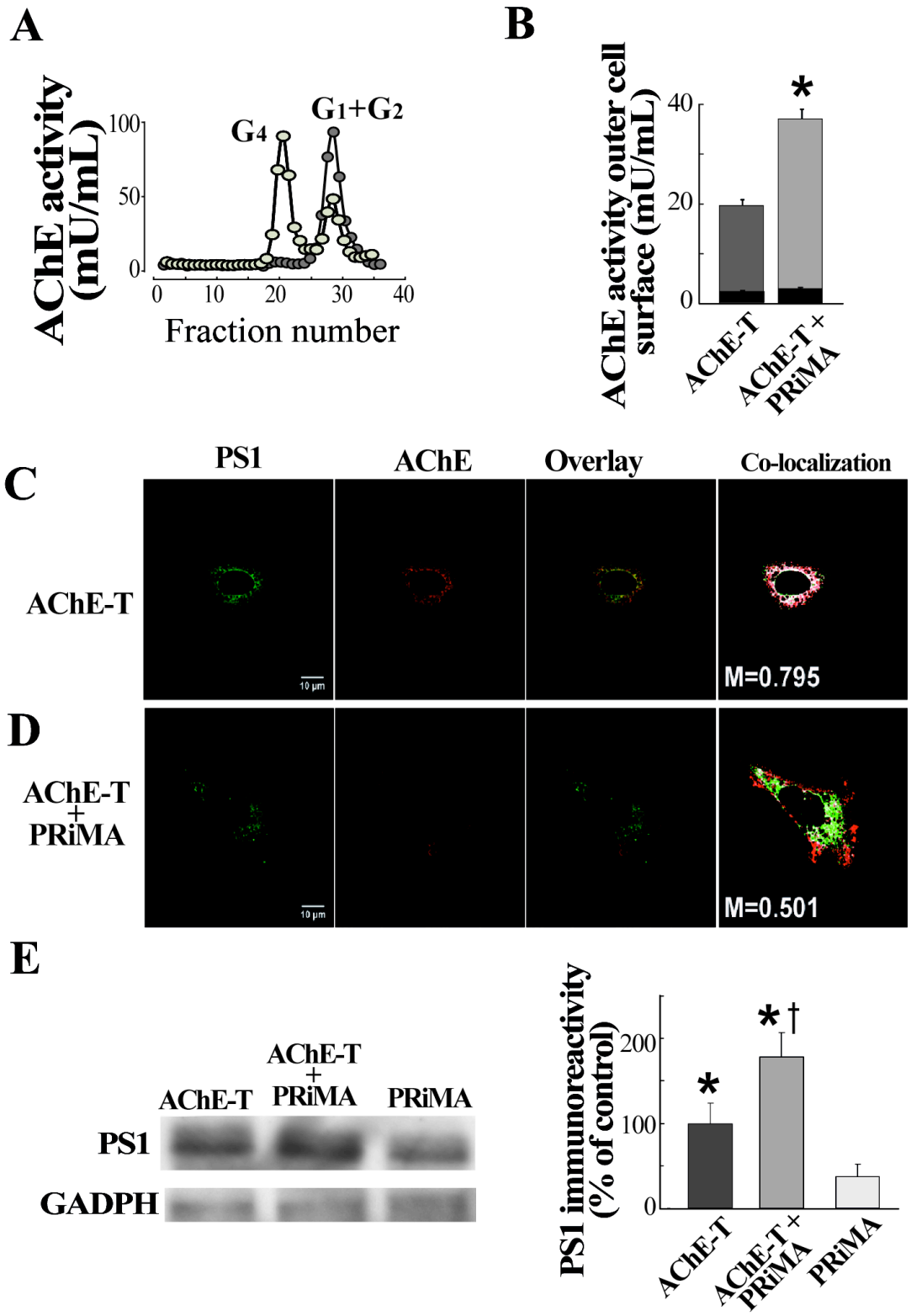

777

778

779 ***Figure 3*. Regulation of PS1 levels by tetrameric PRiMA-linked AChE located in**

780 **the plasma membrane**. (**A**) Representative profiles of AChE in CHO cells stably

781 transfected with AChE-T cDNA without (●; AChE-T) and with PRiMA co-expression

782 (●; AChE-T+PRiMA) (G_4=tetramers; G_1+G_2=monomers and dimers). The results were
783 confirmed in four independent determinations. (**B**) AChE activity was also assayed
784 directly in plasma membranes from cultured cells transfected with AChE-T in presence
785 or absence of PRiMA cDNA. The inner dark columns represent AChE activity levels
786 after treatment with the AChE inhibitor tacrine (10μM). (**C, D**) AChE-T is transported
787 from the cytoplasm to the cell periphery in the presence of PRiMA. Representative
788 images of CHO cells transiently co-expressing PS1 and AChE-T (C), or PS1, AChE-T
789 and PRiMA (D). PS1; PS1-GFP (488 nm) channel, AChE; Anti-AChE N19 (647 nm)
790 channel. Overlay; overlay of 488 nm and 647 nm channels. Co-localization; channel
791 overlay with pixels positive for both PS1 and AChE, marked in white. M; Mander's co-
792 localization co-efficient. Localization of PS1 and AChE-T in the absence of PRiMA is
793 observed mainly in the cytoplasmic region (**C**). The mean number of AChE-T pixels co-
794 localizing with PS1 was 79.5% (n=3). Cells expressing AChE-T+PRiMA and PS1 show
795 localization of AChE at the cell periphery with only 50.1% of AChE pixels co-localized
796 with PS1 (n=3). (**E**) Immunodection and densitometric quantification of PS1-NTF
797 (normalized to GADPH) in CHO cells transfected with AChE-T, AChE-T+PRiMA or
798 PRiMA alone. Columns represent mean ± SEM from two different experiments (n= 10
799 for each condition). Significantly different ($p < 0.05$) from cells over-expressing
800 PRiMA alone (*), or from the AChE-T cells (†).
801

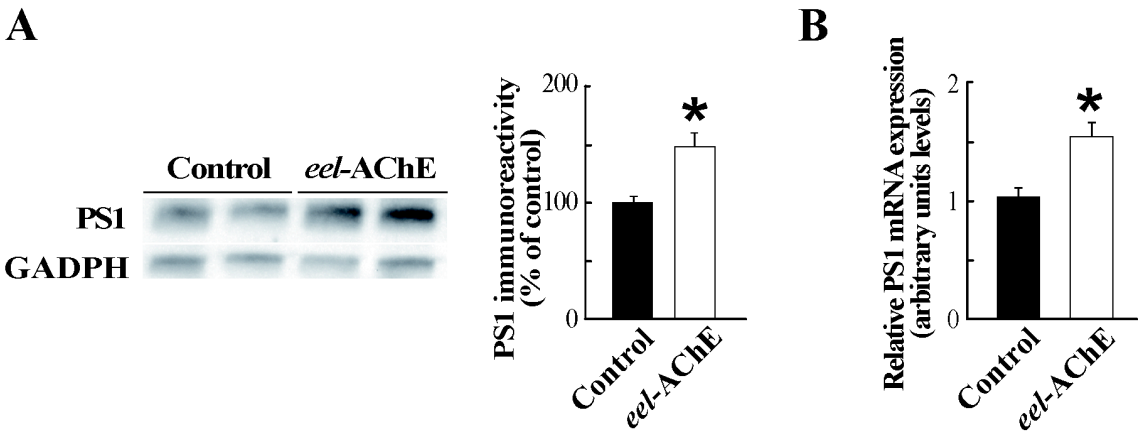

802

803

804 ***Figure 4*. The presence of exogenous AChE increases PS1 expression.** CHO cells
805 were treated for 18 hours with AChE from *Electrophorus electricus* (*eel*-AChE; at
806 ~34±1 mU/mL of enzymatic activity) or saline (Control). (**A**) Cell extracts were
807 analyzed by Western blot with an anti-N-terminal PS1 antibody. Equivalent amounts of
808 protein were loaded in each lane and GAPDH was used as a loading control. An
809 increase in PS1 immunoreactivity was observed in cells treated with *eel*-AChE (**B**)
810 Messenger RNA levels of the PS1 transcript were measured by *q*RT-PCR from cell
811 extracts. Values were calculated using relative standard curves and normalized to
812 GAPDH obtained from the same cDNA preparations. mRNA levels were significantly
813 increased in cells treated with *eel*-AChE. Data represent mean ± SEM from a minimum
814 of 15 independent determinations from three independent experiments. *$p < 0.001$.

815

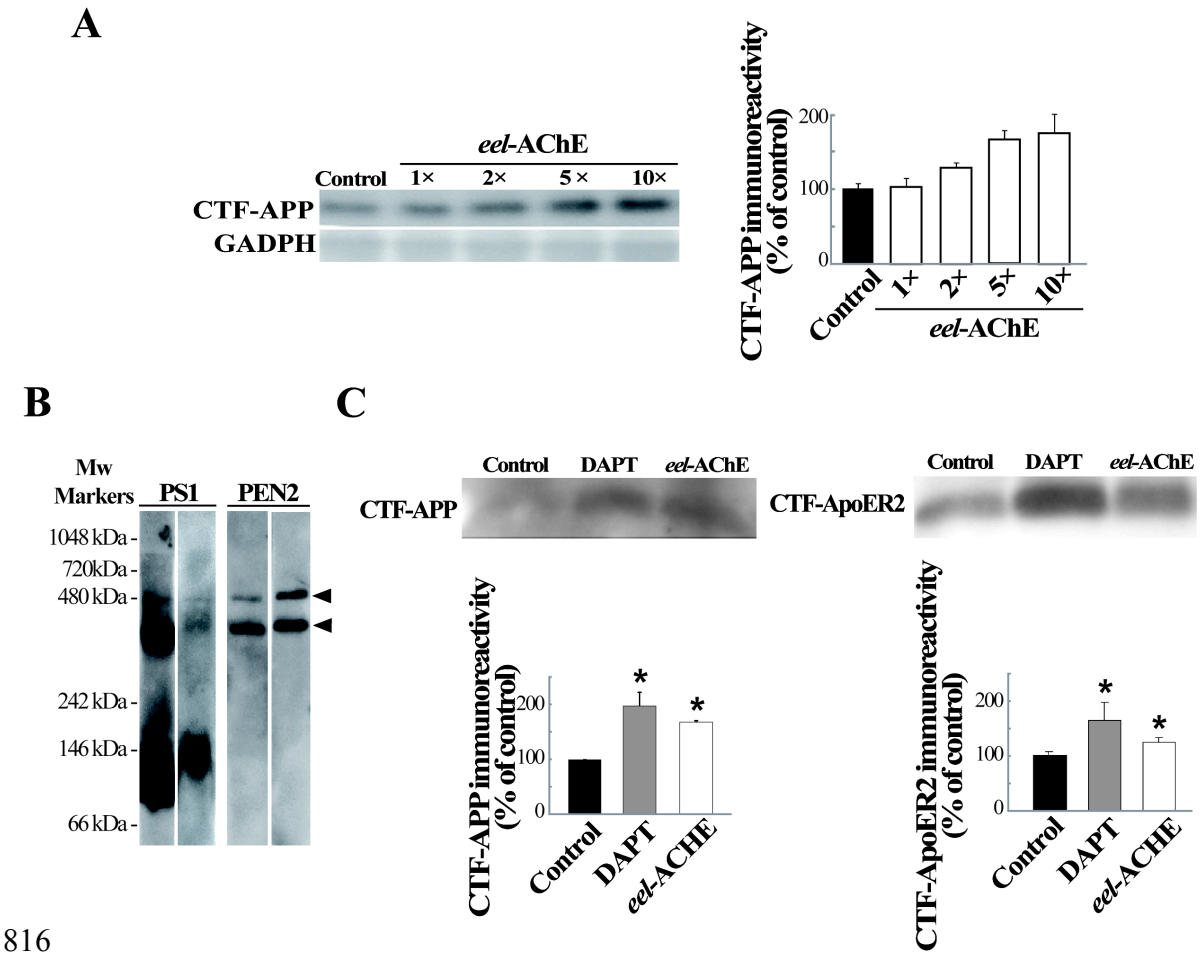

816

817

818 ***Figure 5*. Inhibition of PS1/γ-secretase processing of C-terminal fragments of APP**

819 **by AChE.** (**A**) Dose-dependent effect of soluble AChE from *Electrophorus electricus*

820 (*eel*-AChE) on APP processing. CHO cells were treated with 0 (saline; Control), ~9±1

821 mU/mL (1×), ~17±1 mU/mL (2×), ~34±1 mU/mL (5×) or ~70±1 mU/mL (10×) of

822 active *eel*-AChE. Cell extracts blotted with a C-terminal anti-APP antibody

823 demonstrated APP CTF accumulation in treated cells as a result of the inhibition of γ-

824 secretase processing. (**B**) CHO cells over-expressing PS1 were homogenized and

825 membranes isolated by sequential centrifugation (see Material & Methods). γ-Secretase

826 complexes were characterized by blue native-PAGE using an anti-PS1 antibody.

827 Complexes of different molecular mass were detected. Similar immunoreactive bands

828 (arrowheads) were detected for PEN2, a subunit of the γ-secretase complex. (**C**) γ-

Secretase cleavage of endogenous APP in membrane preparations of CHO cells was assessed in the presence of ~34±1 mU/mL of *eel*-AChE. γ-secretase activity was inhibited in cells treated with 5 μM of the γ-secretase inhibitor DAPT. Data represent the percentage relative to control cells. The results were confirmed in two independent experiments (n= 8 determinations). *$p < 0.05$.

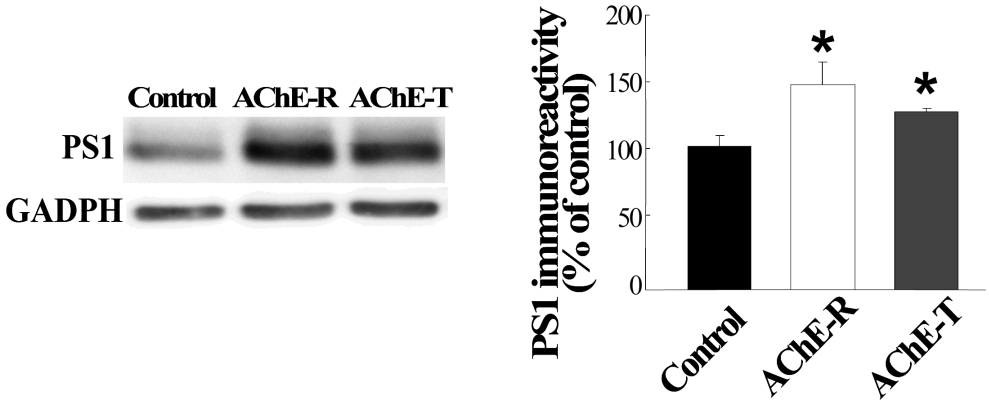

835

836

837 ***Supplementary Figure 1.*** **Effect of the AChE over-expression on PS1 levels in SH-**

838 **SY5Y cells.** Immunodetection and densitometric quantification of PS1-NTF for AChE-

839 R or AChE-T transfected, and control cells transfected with a PCI vector. Protein levels

840 were normalized to glyceraldehyde 3-phosphate deydrogenase (GADPH). Data

841 represent percentage relative to control cells, expressed as means ± SEM of 10

842 independent determinations from at two different experiments. *$p < 0.05$.